Finite element modelling of fabric compression



2008 Modelling Simul. Mater. Sci. Eng. 16 035010

(http://iopscience.iop.org/0965-0393/16/3/035010)

Modelling Simul. Mater. Sci. Eng. **16** (2008) 035010 (16pp) doi:10.1088/0965-0393/16/3/035010

# Finite element modelling of fabric compression

**Hua Lin**[1], **Martin Sherburn, Jonathan Crookston, Andrew C Long, Mike J Clifford and I Arthur Jones**

School of Mechanical, Materials and Manufacturing Engineering, University of Nottingham, University Park, Nottingham NG7 2RD, UK

E-mail: hua.lin@nottingham.ac.uk

Received 20 December 2007, in final form 21 December 2007
Published 26 March 2008
Online at stacks.iop.org/MSMSE/16/035010

**Abstract**

The mechanical behaviour of woven fabric under compression is investigated using 3D finite element analysis in conjunction with a nonlinear mechanical model for the yarn. The FE model captures the main fabric compression response, including geometric and material nonlinearities, yarn interactions and hysteresis. It is found that the behaviour of fabric in compression is governed by the stiffness of the yarn cross-section and the transverse–longitudinal shear modulus. The stiffness along the yarn direction has no noticeable effect. The model is sufficient to simulate the known responses of a fabric as well as to predict the behaviour of novel fabrics based on the properties of the component yarns and yarn interactions.

(Some figures in this article are in colour only in the electronic version)

## 1. Introduction

Woven fabric materials find numerous important applications ranging from aerospace and textile composites to apparel. In recent years, many cutting-edge studies have focused on certain special-purpose applications of fabrics, such as body armour for ballistic protection [1] and fabric integrated with flexible electronics for communications [2]. Conversely, engineers carefully design fabric architectures to obtain the best possible combination for cost, weight, strength and performance. All these aspects require a thorough understanding of the mechanical behaviour of woven fabrics. There is thus a significant need for modelling of the mechanical behaviour and performance of textiles.

Woven fabrics are made of yarns which are woven in one of several different patterns. Each yarn, in turn, comprises many fibres which are bundled together into a single structure. The material properties of fabric are greatly affected by their underlying microstructure. There

[1] Author to whom any correspondence should be addressed.

  

are many challenging aspects of modelling fabric behaviour, for example, even the geometry of relatively simple plain weave fabrics is complicated and requires careful modelling to obtain realistic results.

The aim of this study is to develop a computational modelling approach for FE analysis of fabric compression. This will be applied subsequently to determine the mechanical behaviour of woven fabric under other loading conditions, such as tension, shear and bending, as well as combinations of these. These simulations are targeted to determine the theoretical dependences of fabric mechanical performance on its component properties and structural parameters, and to identify the primary deformation mechanisms under different loading conditions. The simulations will be used to:

- predict the behaviour of fabrics based on the properties of the component yarns and yarns interactions;
- assist engineers in selecting yarns and fabric structures for specific applications;
- create a database for fabric and fabric-based material optimization;
- enable a virtual fabric design/testing system to reduce cost and lead-time in introducing new textiles;
- predict the results of changes of mechanical and geometric properties of a fabric due to a manufacturing process such as composite forming or automatic material handling;
- provide a detailed understanding of the behaviour of woven fabric under a variety of external loadings to guide the development of analytical modelling.

The focus of this paper is on prediction of woven fabric compression. There has been considerable research in this area both in the textiles and composites literature. Studies generally involve either empirical/semi-empirical analytical modelling or mechanical (finite element based) modelling. There are many challenges to develop analytical models which can accurately capture the important aspects of fabric deformation in compression.

van Wyk [3] derived a relation between pressure and volume for a random wool fibre assembly under hydrostatic compression on the assumption that the compression of the mass resulted only in bending of the fibres. Toll and Manson [4] related applied pressure $P$ to fibre volume fraction $V_f$, using a power law, $P = cV_f^n$, where $c$ and $n$ are empirical constants to characterize the compressibility of random fibre assemblies. van Wyk's model and the power law have been used widely and extended to fit experimental data on textiles and textile composites, as reviewed by Robitaille and Gauvin [5] and Sherburn [6]. Gutowski and Cai developed a theory for the deformation behaviour of aligned fibres suitable for production of composite materials [7,8]. The path of each individual fibre was assumed to follow a sine wave. However, the above models are unable to predict compression properties without empirical parameters. To overcome this limitation, several researchers have employed energy methods to tackle the difficulties in analytical modelling of fabric compression [9,11]. In this method, the deflection of the fibre elements was assumed to be proportional to the compression of the total fibre assembly. The energy required to cause this deflection was added for all fibres to obtain the total energy for fabric compression. The results of this method were not compared with experimental data. Lee and Carnaby [12, 13] conducted a similar study on uniform random assemblies of fibres using an energy method; however, this method was not applied to aligned fibre assemblies.

On the other hand, by taking advantage of the hierarchical nature of fabrics, several researchers related applied pressure to preform thickness by modelling yarn deformations [14, 15]. They treated a yarn as an elastic beam and employed beam bending theory to model deformation in compaction of woven fabrics. In Chen and Chou's model [14], the yarn cross-section shape can deform, but the yarn cross-sectional area (and thus its fibre packing state)

remains unchanged during compaction. In that case the compaction of a single layer of woven fabric is attributed to yarn waveform flattening deformation only. In contrast, Lomov *et al* [15] described a predictive model, based on detailed yarn mechanical characterization data. This included yarn compression and deformation of the yarn waveform (yarn flattening). Reasonable agreement was reported between experimental compaction data and predictions for two plain weave fabrics, although it was noted that accuracy of fabric geometry predictions may be limited by inability to model yarn widening. The model proposed by Chen *et al* [16] considered not only the two deformation mechanisms (compression of yarns and change of yarn crimp) but also the surface area on which the externally applied load acts, as well as the interaction area of between yarn crossovers. However, in Chen *et al*'s model, yarn compaction was modelled using Gutowski's model [7] and yarn waveform flattening was also considered via a simple fibre bending model. This was applied to a variety of woven fabrics, and good agreement with experimental data for a plain weave fabric was reported by selecting an appropriate value for the empirical fibre waviness parameter. Additionally, a common limitation of the above models is that the friction between yarns and friction between fibres within a yarn are ignored. Energy dissipation due to the friction is one of the most important mechanical behaviours of fabric in compaction, especially for dry fabrics [17].

The use of the three-dimensional finite element method allows better modelling of the complex weave geometry and the spatially varying properties of the yarn. However, a realistic description of the weave geometry and the development of appropriate material models can also be formidable challenges. At present no published studies exist on this topic.

A great deal of research has been performed on analysing the compression behaviour of fibre assemblies. However, there has been no general detailed modelling study of fabric compression. The aims of this study are to model woven fabric compression behaviour, including geometric nonlinearities, material nonlinearities, energy dissipation due to friction and dependences of fabric mechanical performance on its component properties and structural parameters.

The organization of this paper is as follows: section 2 describes in detail the proposed unit cell fabric model, including geometric modelling and material modelling. Modelling of fabric in compression is discussed in section 3, focusing on the contributions of geometric nonlinearities and material nonlinearities, followed in section 4 by an investigation of the significance of different parameters on fabric compression response.

## 2. Model development

### *2.1. Geometric modeling*

Fabric unit cell geometries were generated using TexGen[2], in-house software, which is described in detailed in [6]. Here, a brief description is given of how the unit cell geometries were generated for a glass fibre plain weave (Chomarat 150TB) and a satin weave (Chomarat 800S4-F1).

*2.1.1. Yarn path.* In TexGen, the yarn path is represented by the yarn centre line in three-dimensional space. Thus the yarn path is defined as position in 3D space as a function of distance along the yarn. The most flexible and generic way to describe such a yarn path is to specify a number discrete positions along the length of the yarn, known as master nodes, and to interpolate between these points. Generally, to obtain an accurate yarn path for woven fabrics

[2] TexGen is available as open source at http://texgen.sourceforge.net/

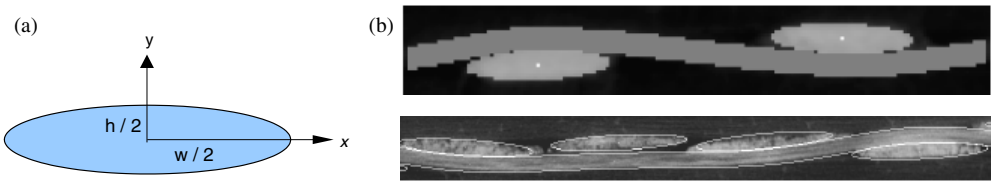


**Figure 1.** Elliptical yarn cross-section assumed (*a*), $\mu$CT analysed (*b*) Chomarat 150TB (top), Chomarat800S4-F1 (bottom).

it is sufficient to specify one or two master nodes per crossover as long as the interpolation function is suitable. The interpolation function must have at least continuity $C^1$, i.e. there are no gaps in the yarn path and the tangent varies smoothly along the length of the yarn. A common solution to this problem is to use splines (piecewise polynomial functions). In its most general form a polynomial spline $S : [a, b] \to R$ consists of polynomial pieces $P_i : [t_i, t_{i+1}) \to R$, where

$$a = t_0 < t_1 < \cdots < t_{k-2} < t_{k-1} = b. \tag{1}$$

That is,

$$\begin{aligned} S(t) &= S_0(t), && t_0 \leqslant t < t_1, \\ S(t) &= S_1(t), && t_1 \leqslant t < t_2, \\ &\cdots\cdots \\ S(t) &= S_{k-2}(t), && t_{k-2} \leqslant t \leqslant t_{k-1}. \end{aligned} \tag{2}$$

The given $k$ points $t_i$ are called knots. The vector $t = (t_0, \ldots, t_{k-1})$ is called a knot vector for the spline. In this study, b-splines were used to represent yarn centre-lines for the two weaves.

*2.1.2. Yarn cross-section.* The yarn cross-section is defined as the 2D shape of the yarn when cut by a plane perpendicular to the yarn path tangent. In TexGen, yarns are treated as solid volumes and the cross-section is approximated to be the smallest region that encompasses all of the fibres within the yarn (it will generally be convex). The outline of the cross-sections can be defined using 2D parametric equations. Various shapes can be used to accurately represent the cross-sectional shape of a yarn.

In this study, the yarn cross-section for the plain weave and the satin weave is modelled as an ellipse which was validated using x-ray microtomography ($\mu$CT) analysis [6] as shown in figure 1. An ellipse can be mathematically described as

$$C(t)_x = \frac{w}{2}\cos(2\pi t) \qquad 0 \leqslant t \leqslant 1, \tag{3}$$

$$C(t)_y = \frac{h}{2}\sin(2\pi t) \qquad 0 \leqslant t \leqslant 1, \tag{4}$$

where $w$ is the width of yarn cross-section, $h$ is the height of yarn cross-section.

*2.1.3. Yarn surface.* After the yarn path and cross-section are defined, the two need to be brought together. The yarn is usually uneven, thus the cross-section of yarn should be defined as a function of distance along the yarn. TexGen implements a simple geometric algorithm to deal with this issue, starting with an elliptical geometry which is modelled locally to avoid interference between yarns volumes [6].

**Table 1.** Unit cell geometry.

| | Yarn spacing (mm) | Yarn width (mm) | Fabric thickness[a] (mm) |
|---|---|---|---|
| Chomarat 150TB plain weave | 1.66 | 0.82 | 0.30 |
| Chomarat 800S4-F1 satin weave | 3.16 | 3.16 | 1.16 |

[a] Thickness at pressure of 5 gf cm$^{-2}$.

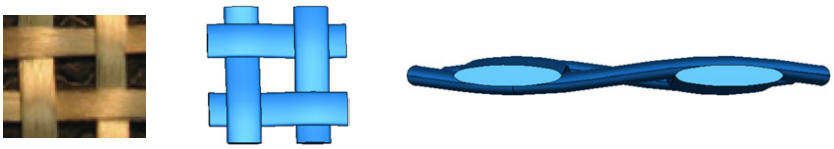

**Figure 2.** Chomarat 150TB (left), modelled unit cell (middle and right).

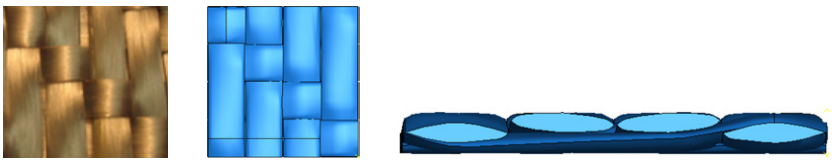

**Figure 3.** Chomarat 800S4-F1 (left), modelled unit cell (middle and right).

**Table 2.** Material properties.

| | Areal density (g m$^{-2}$) | Fibre density (g cm$^{-3}$) | Total yarn volume (mm$^3$) | Volume of fibres (mm$^3$) | Fibre volume fraction of yarn (%) |
|---|---|---|---|---|---|
| Chomarat 150TB plain weave | 150 | 2.62 | 1.38 | 0.74 | 0.55 |
| Chomarat 800S4-F1 satin weave | 780 | 2.62 | 115.6 | 47.54 | 0.41 |

*2.1.4. Unit cell.* The fabric thickness was measured using the Kawabata Evaluation System for Fabrics (KES-F) [18] at a pressure of 5 gf cm$^{-2}$. Yarn width and yarn spacing were measured by ruler rounded to two decimal places. In addition, based on the manufacturers' specification the two weaves are assumed to be balanced, i.e. both the warp and weft have the same geometric and material properties. The measured and modelled fabric geometric parameters are given in table 1. The fabric unit cells of the plain weave and the satin weave and the corresponding unit cells generated by TexGen are shown in figures 2 and 3.

Table 2 gives the material properties of the two weaves. The areal density of the fabric was obtained from the manufacturer's data sheet, and the density of E-glass fibres was obtained from Reinhard *et al* [19]. The yarn volume was calculated from the geometric model. Fibre volume fraction $V_f$ was calculated by

$$V_f = \text{total yarn volume/fibre volume}.$$

### *2.2. Material modelling*

*2.2.1. Linear elastic orthotropic material model.* In this study, yarns are modelled as continuum solid bodies. In a continuum description, the yarn is treated as an orthotropic material. The longitudinal direction is defined by 11, which is parallel to fibres; the transverse plane is described by the directions 22 and 33, which are characterized by a plane of isotropy at every point in the material.

The orthotropic behaviour of the yarn is typically described using a 3D stiffness matrix containing nine independent constants [20]:

$$\begin{bmatrix} \varepsilon_{11} \\ \varepsilon_{22} \\ \varepsilon_{33} \\ \varepsilon_{23} \\ \varepsilon_{13} \\ \varepsilon_{12} \end{bmatrix} = \begin{bmatrix} \frac{1}{E_{11}} & -\frac{\nu_{12}}{E_{11}} & -\frac{\nu_{13}}{E_{11}} & 0 & 0 & 0 \\ -\frac{\nu_{12}}{E_{11}} & \frac{1}{E_{22}} & -\frac{\nu_{23}}{E_{22}} & 0 & 0 & 0 \\ -\frac{\nu_{13}}{E_{11}} & -\frac{\nu_{23}}{E_{22}} & \frac{1}{E_{33}} & 0 & 0 & 0 \\ 0 & 0 & 0 & \frac{1}{G_{23}} & 0 & 0 \\ 0 & 0 & 0 & 0 & \frac{1}{G_{13}} & 0 \\ 0 & 0 & 0 & 0 & 0 & \frac{1}{G_{12}} \end{bmatrix} \begin{bmatrix} \sigma_{11} \\ \sigma_{22} \\ \sigma_{33} \\ \sigma_{23} \\ \sigma_{13} \\ \sigma_{12} \end{bmatrix}. \quad (5)$$

The yarn is transversely isotropic, hence

$$E_{22} = E_{33}, \qquad \nu_{12} = \nu_{13}, \qquad G_{12} = G_{13}.$$

When loading starts, the fabric is compressed, and the cross-sectional shape of the yarn changes as the yarn itself is compacted. Hence, the longitudinal Young's moduli and shear moduli of the yarn increase with increasing fibre volume fraction.

The longitudinal modulus $E_{11}$ can be approximated as a linear function of fibre volume fraction $V_f$ of a yarn [20] and fibre modulus $E_f$ by the following equation:

$$E_{11} = E_f V_f. \quad (6)$$

This assumes all fibres within a yarn are perfectly parallel and hence no stiffening of the yarn occurs due to fibre straightening at low strains.

In this study, for simplicity a constant $E_{11}$ ($E_{11} = E_f V_{f0}$, $V_{f0}$ is initial fibre volume fraction of the yarn) was used in the simulations.

The yarn transverse–longitudinal shear behaviour is governed mainly by the sliding of fibres relative to each other. As such this cannot accurately be represented by an elastic modulus $G_{13}$ alone. There are no experimental data available for yarn transverse–longitudinal shear modulus. McBride assumed that the longitudinal shear modulus is proportional to the transverse shear modulus by a constant of proportionality set to a value of 2 with no further explanation [21]. Boisse *et al* [22] used a small value for the property but they did not specify the value used in plain weave glass fabric tensile FE modelling. This issue is explored later in this study.

*2.2.2. Nonlinear material behaviour.* The transverse stiffness, $E_{33}$ ($E_{22} = E_{33}$), increases during compaction as the gaps between fibres are reduced. Finally, the stiffness tends to an asymptotic value, which is very large in comparison with that at low strain. It has been shown

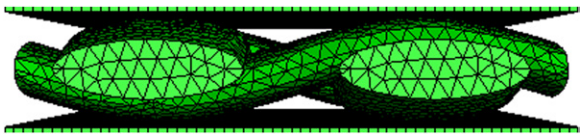

**Figure 4.** Simulation set-up for plain weave unit cell compression.

that the compaction curve of pressure, $P$, versus fibre volume fraction, $V_f$, can be approximated by a power law requiring only two fitting parameters, $a$ and $b$ [4]:

$$P = aV_f^b. \tag{7}$$

In order to create a constitutive material model based on equation (7), it is necessary to convert it into a relationship between stress and strain, providing modulus $E_{33}$ as a function of strain. The details of this procedure are described in [6]. The result is

$$E_{33}(\varepsilon_{33}) = \frac{\sigma_{33}}{\varepsilon_{33}} = \frac{-a(V_{f0}/e^{\varepsilon_{33}})^b + a(V_{f0})^b}{\varepsilon_{33}}. \tag{8}$$

The initial value of $E_{33}$ is

$$E_{33}(0) = \lim_{\varepsilon_T \to 0} \frac{\sigma_T}{\varepsilon_T} = \frac{d\sigma_T}{d\varepsilon_T} = ab\left(\frac{V_{f0}}{e^{\varepsilon_{33}}}\right)^b, \tag{9}$$

where $V_{f0}$ is initial fibre volume fraction; $a$ and $b$ are experimentally determined parameters. The parameters $a$ and $b$ in the expression may exhibit dependence on the fabric state. In the current model implementation, these parameters are considered as constant material properties, with values $a = 1151$, and $b = 12.24$ obtained by fitting McBride's E-glass yarn compression data [21] using the power law (equation (7)).

Due to the transverse isotropy, the transverse shear behaviour is characterized by

$$G_{23} = \frac{E_{33}}{2(1 + \nu_{23})}. \tag{10}$$

The constitutive yarn models (equations (8) and (10)) have been implemented into ABAQUS/Standard, an implicit finite element code, through a user-defined material subroutine (UMAT).

### *2.3. FE implementation*

The plain weave and the satin weave unit cells were discretized using 8818 and 32384 4-noded tetrahedral three-dimensional continuum elements, respectively. The predictions were practically insensitive to further refinement in mesh density. Two compression platens were created using rigid elements with steel properties ($E = 200$ GPa and Poisson's ratio $= 0.3$). The unit cell was placed between the two platens as shown in figure 4. The lower platen was fully constrained. Compression was applied at a constant displacement rate of the upper platen. The initial platen separations were 0.302 mm and 1.19 mm for the plain weave and the satin weave simulations, respectively, as used in experimental studies for validation. Due to geometrical nonlinearities, the model is analysed according to large strain theory, i.e. the nonlinear geometry option was used. Node sets were generated at the ends of each yarn. Tie constraints were applied to the node sets using a master–slave surface approach to implement periodic boundary conditions to reflect the repeating nature of woven fabric. Multiple contacts were defined between yarns and the unit cell surfaces with the platens using the surface–surface

**Table 3.** Input data for geometric nonlinearity simulations.

| | $E_{11}$ (MPa) | $E_{33}$ (MPa) | $G_{12}$ (MPa) | $G_{23}$ (MPa) | $\nu_{12}$ | $\nu_{23}$ |
|---|---|---|---|---|---|---|
| Plain | 40150 | 75 | 5 | 31.25 | 0.2 | 0.2 |
| Satin | 29930 | 15 | 5 | 6.25 | 0.2 | 0.2 |

approach. Average frictional coefficients (0.3) and (0.5) were chosen from testing results for contacts between yarns and yarns with the platens, respectively [23].

An automated modelling approach developed by Crookston *et al* [24] has been employed in this study. A Python scripting interface was created to enable TexGen textile models to be reproduced within a mechanics modelling environment in an automatic way. The unit cell geometry generated by TexGen is saved and the script reads the file. Subsequently, the script loops over the textile hierarchy and retrieves the geometric data defining the outer surfaces of the yarns. These points are used for lofting solid yarn bodies within Abaqus/CAE. Subsequently, operations are incorporated which perform Boolean subtraction to trim yarns to a single unit cell and to generate the platens, and to define materials and boundary conditions as well as contact between the yarns and the platens. Mesh generation operations are also undertaken in the script. The script creates a job which is submitted for analysis.

Simulations were performed for the following properties:

1. unit cell compression with a linear elastic orthotropic material model (equation (5));
2. unit cell compression incorporating nonlinear transverse behaviour (equations (8) and (10));
3. unit cell compression with different yarn mechanical properties and geometries.

## 3. Modelling of fabric compression

### *3.1. Geometric nonlinearity*

A set of uniaxial deformations were applied in order to assess the geometric response. Here, the material parameters for the unit cell model were specified as in table 3. Longitudinal modulus, $E_{11}$, was calculated using equation (6), using $E_f = 73$ GPa. $E_{33}$ was simply selected to achieve a reasonable comparison with experimental results. Data for the yarn transverse–longitudinal shear behaviour, $G_{12}$ ($G_{12} = G_{13}$), were not available in the literature, hence a small value (5 MPa) was used. A Poisson's ratio of 0.2 for both transverse and longitudinal directions of the yarns was selected from the literature [25].

Compression tests on the plain weave and the satin weave were carried out on standard testing equipment (Hounsfield). Fabrics were compressed between two parallel plates, with force measured using a load cell and displacement measured using a displacement transducer (LVDT).

A comparison between the predicted and measured pressure–strain curves is given in figure 5 for the plain weave and the satin weave using the linear material model, i.e. the six engineering constants. Strains were calculated from displacement divided by unit cell thickness. This figure shows that the linear elastic orthotropic material model is suitable for the first deformation/small load regime only, as expected. Geometric nonlinearity effects alone are significant in the compression response of the two weaves. These effects arise from the undulation of the yarns and are a significant factor in compressive behaviour. However this is not enough on its own to characterize fabric compression behaviour; proper modelling of the material nonlinearity is essential.

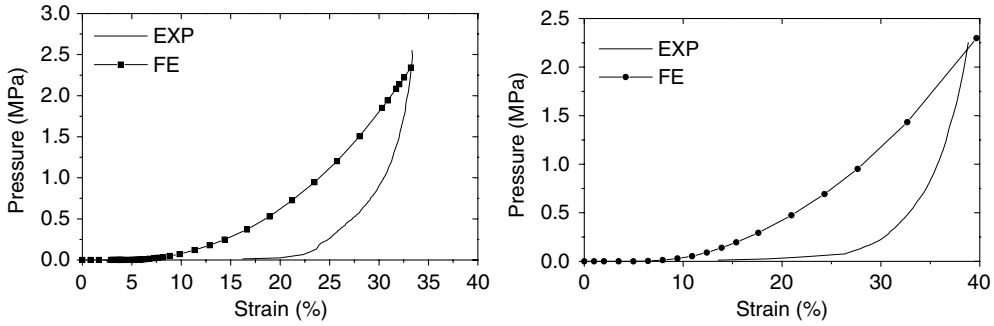


**Figure 5.** Comparison between experimental data and FE analysis for a plain weave (left) and satin weave (right) using the linear material model.

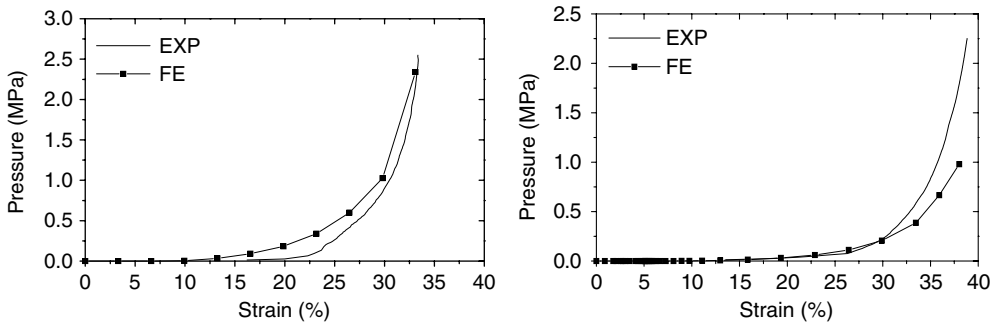


**Figure 6.** Comparison between experimental data and FE analysis for the plain weave (left) and the satin weave (right) using the nonlinear material model.

### *3.2. Material nonlinearity*

Using equations (8) and (10) to calculate $E_{33}$ and $G_{23}$ separately, figure 6 shows that the nonlinear material model gives an improved prediction of the pressure–strain behaviour of both woven fabric unit cells. Comparison between figures 5 and 6 indicates that nonlinearity of yarn compression is predominant, while the geometric changes and contact nonlinearity are also important. It should be noted that no curve fitting was required to obtain the agreement displayed in figure 6. All properties were taken from table 3, apart from $E_{33}$ which was based on published yarn compaction data as described in section 2.2.2.

### *3.3. Localized deformation*

The simulated deformed unit cells for the plain weave and the satin weave are shown in figure 7. Contact stresses in crossover regions are shown in figure 8.

In the case of fabric compression, the stress is localized in a small area in contact with the upper platen. This, in fact, shows that the capability of the fabric to sustain loads is limited by this localized behaviour. In compression, the central part of the yarn cross-section carries the load. First a flat region is developed on a yarn cross-section in two component yarns (figure 7), and as a result the cross-section deforms and the yarn is compacted. At this time the two side parts of the yarn cross-section deform due to the action of lateral compression, but no compaction occurs in these areas because the fibres do not carry any load. The deformed

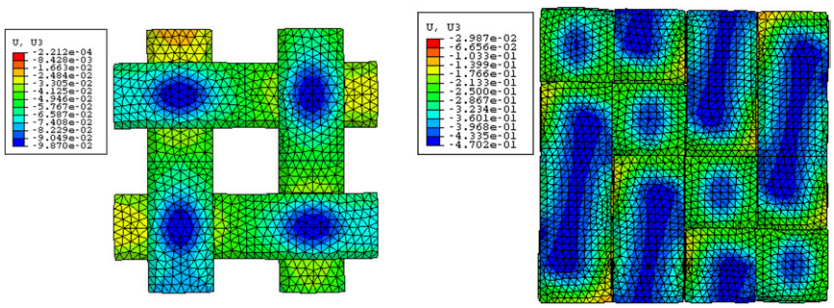


**Figure 7.** Predicted displacement distribution in the unit cells (left) plain weave, (right) satin weave.

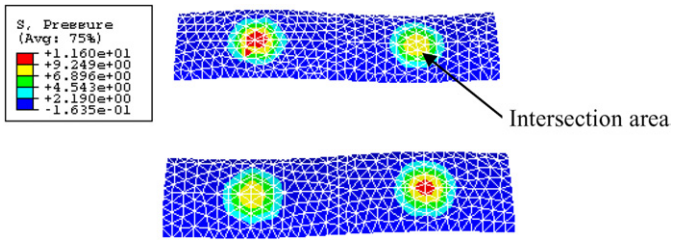


**Figure 8.** Predicted pressure (MPa) distribution in yarn contact regions for the plain weave.

cross-section is assumed to have different fibre volume fraction in different areas. The fibre volume fraction of the contact area of the central region, $V_f$, increases during the process of compaction, while that at the yarn edges remain at the initial fibre volume fraction, $V_{f0}$.

The compressive force is not evenly distributed between regions of warp–weft contacts (figure 8). Compressive force acting on yarns is distributed over a small area of warp–weft contacts, while the area of the contact region is dependent on the geometry and mechanical properties of the yarns, as well as the loading condition.

These simulations reveal that during compaction, not all the sections of a yarn carry the same load simultaneously, and only those at yarn crossovers carry the external load. The external load is equivalent to the internal forces acting on the fabric mesostructural components (yarns). These forces are due to yarn tension, yarn bending moments, moments between yarns and contact forces. However, which internal forces dominate the deformation depends on the loading conditions. In the case of unit cell compression, yarn bending and compression are thought to have a significant effect on the global deformation [26, 27]. The change in fabric thickness arises from yarn compression and changes in yarn crimp. The compression force changes the dimensions of compressed yarn cross-sections and changes the yarn crimp height, leading to fabric thickness reduction.

Additionally, the area for carrying external load for the satin weave is greater than that of the plain weave, i.e. the compressive force is distributed in larger regions of warp–weft contacts for the satin weave. This could be one of the reasons why the satin weave is more compliant (see figure 6).

### *3.4. Energy dissipation*

The whole system energy and strain energy are plotted in figure 9 for the plain weave model. The strain energy is obtained as the sum of the energies of all elements within the unit cell,

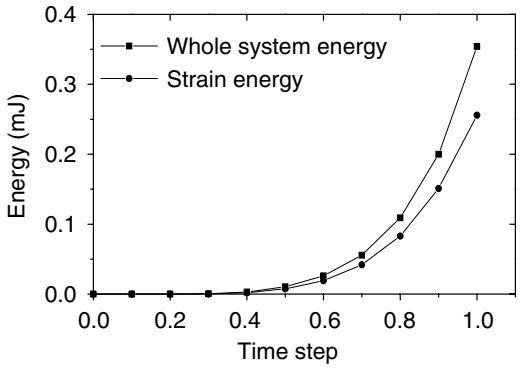


**Figure 9.** Energy in the system for plain weave unit cell compression.

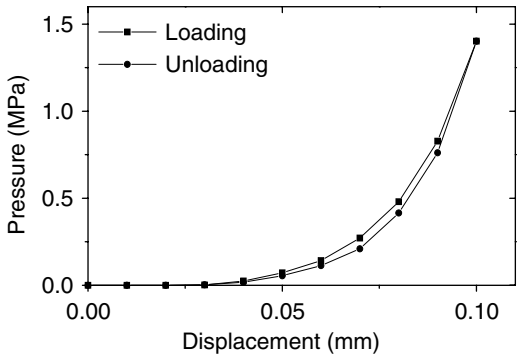


**Figure 10.** Predicted loading and unloading cycle for plain weave.

comprising yarn tension, compression, shearing and bending. The compaction of a single layer of woven fabric involves two important deformation mechanisms, yarn cross-section deformation and compaction and yarn bending deformation accompanied by yarn flattening. Hence, compression strain energy is mainly from yarn compression and yarn bending. Within the high-stress deformation regime, the energy associated with yarn bending is small compared with that associated with yarn compression. The contribution of bending deformation to compression is mainly from the free zones.

The difference between external whole system energy and strain energy is due to friction dissipation between yarns. Friction dissipation is also shown in a loading and unloading cycle (figure 10). In comparison with experimental data [17], friction dissipation is underestimated as friction between fibres within yarns was not included in the simulation due to yarns being modelled as continua. A more sophisticated yarn model, which models inter-fibre friction, is needed to accurately predict hysteresis in fabric compression behaviour.

## 4. Parametric study

To evaluate the influence of material and geometric parameters on the overall mechanical behaviour of the unit cell in compression, a parametric study was carried out for the plain weave model.

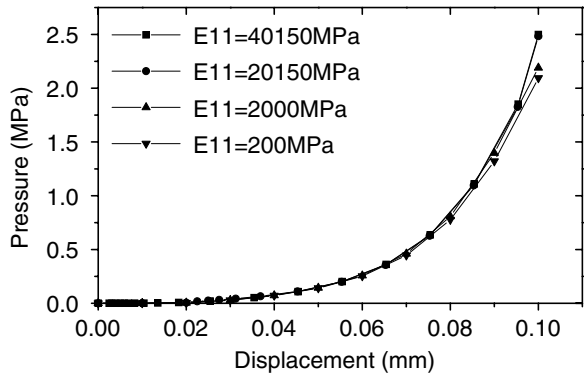


**Figure 11.** Effect of $E_{11}$ on plain weave unit cell compression.

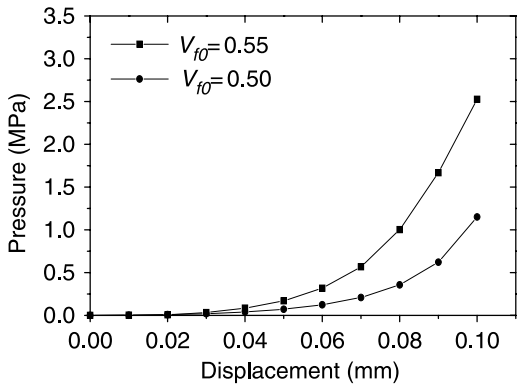


**Figure 12.** Effect of $E_{33}$ on plain weave unit cell compression.

### *4.1. Effect of material properties*

A set of nonlinear elastic uniaxial deformations was applied in order to assess the dependence of material compression on stiffness in different directions.

Figure 11 shows that variation of $E_{11}$ has no effect within a large range of values. This is due to the fact that material behaviour and loading conditions both determine the response of the material. Here the compressive load causes the through-thickness strain to be much greater than in the longitudinal direction (no external loading in the longitudinal direction). The material used in this study is strongly orthotropic, i.e. the stiffness in the longitudinal direction is much greater than that transverse to the yarn, consequently, the longitudinal strain is negligible. The assumption that the compression property is independent of the tension is reasonable at low load range as described in Kawabata's analytical modelling [28].

Figure 12 illustrates the effect of using different initial fibre volume fractions ($V_{f0}$) in equation (8). This shows that the transverse Young's Modulus, $E_{33}$, dominates the compressive behaviour of the fabric, as expected.

In the material law for an orthotropic material, equation (5), there are no coupled terms in the stress–strain relationship. If a load is applied in three principal directions on a straight yarn, there is no shear deformation. However, in the simulations, the yarns are not only

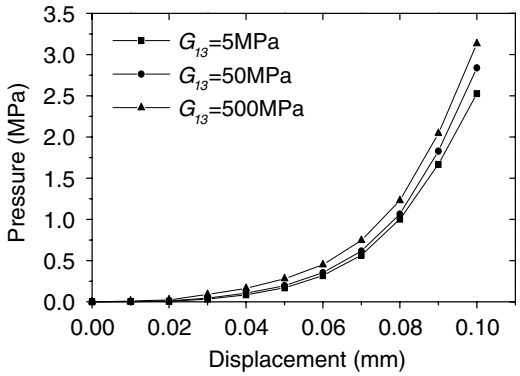


**Figure 13.** Effect of $G_{13}$ ($G_{13} = G_{12}$) on plain weave unit cell compression.

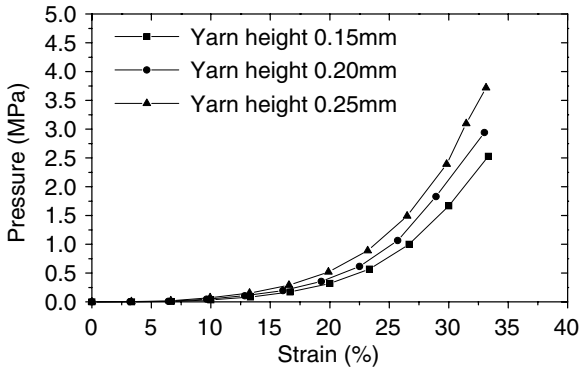


**Figure 14.** Effect of yarn height on plain weave unit cell compression.

in compression but also in shear. This is because the yarns are curved. Consequently, the transverse–longitudinal shear modulus influences the compression behaviour as shown in figure 13. However it is clear that the dependence is relatively weak and that yarn compression is by far the most important mechanism.

### *4.2. Effect of yarn shape*

The relationships between yarn height and pressure are shown in figure 14 using the nonlinear material model and keeping other parameters constant. The model with greatest yarn height was shown to be the most difficult to compact, while the thinnest unit cell was easiest to compact. The physical basis for this result is that the yarns were modelled as elastic orthotropic solid bodies. Hence the thicker yarns have greater bending rigidity and the meso-bending deformation of the yarn physically contributes much less to resisting macro unit cell compaction. Consequently, the fabric compressibility can be reduced when the yarn height is increased.

Moreover, the yarn height directly influences yarn crimp interchange which is important since this directly affects the in-plane stiffness and the geometric nonlinearity. The yarn crimp amplitude increases with increasing yarn height, and consequently the pressure–displacement

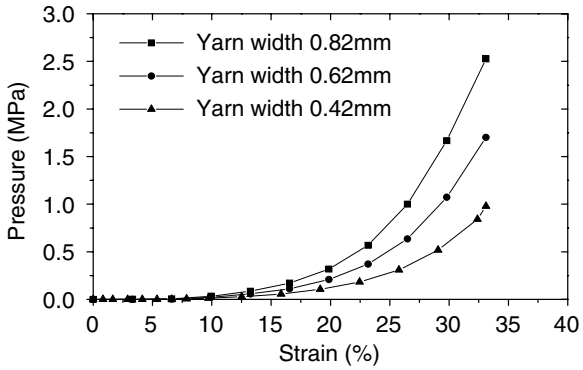


**Figure 15.** Effect of yarn width on plain weave unit cell compression.

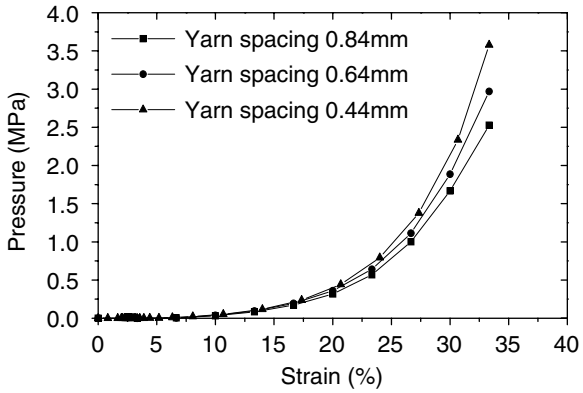


**Figure 16.** Effect of yarn spacing on plain weave unit cell compression.

response contains a larger average geometric nonlinear response. The thinner yarn gives a smaller average effect of geometric nonlinearity.

The influence of varying yarn width is shown in figure 15 under the same yarn spacing and height. Fabric with wider yarns is stiffer for two reasons. From the mechanics viewpoint, the bending rigidity increases linearly with yarn width. From the geometric point of view, the contact area at crossovers increases with increasing yarn width. The yarn meso-bending deformation will dominate the compressive behaviour of the unit cell when the yarn width is sufficiently small.

### *4.3. Effect of yarn spacing*

Clearly, due to meso-bending deformation, the contribution of the curved yarn segment to compaction of the unit cell is quite different from that of the straight segment. Thus unit cells with larger yarn spacing are more compliant due to a higher ratio of free segment to contact region. The meso-bending deformation of the yarn physically contributes much more to compaction resistance, which results in greater capacity to resist compression as shown in figure 16.

## 5. Discussion and conclusions

A FE unit cell compression model has been developed for woven textiles. One of its major advantages over other approaches is that it is able to capture the most important characteristics of the material under compressive loading. Nonlinear geometric and nonlinear material behaviours are the most important features to be modelled. Yarn compaction and, to a lesser extent, yarn bending deformations are the main mechanisms which influence the compaction behaviour.

The model results have confirmed that unit cell compression behaviour is controlled by the transverse yarn stiffness and transverse–longitudinal shear behaviour. Yarn longitudinal stiffness has essentially no influence. Friction between yarns has a small effect during cyclic loading. The compression behaviour of a unit cell also depends on yarn shape and yarn spacing. These findings could inform analytical modelling development and, ultimately, textile design.

Although the model presented here is able to capture the most important responses of a unit cell to compressive loading, a fundamental issue is that the yarn was modelled as a continuum solid body which is unable to accurately capture real yarn deformation mechanisms. A yarn is a bundle of fibres. The meso-bending and shearing behaviour and cross-section compaction behaviour of the yarn are very complex. The internal fibre strains cannot be correctly represented by traditional continuum elements. Development of a finite element which can capture the internal fibre strains either by replacing continuum elements or by working in conjunction with them may solve the issue. This may be achieved, for example, by embedding truss elements inside continuum elements to represent each individual fibre or a group of fibres. The truss elements could represent the tensile and flexural modulus of the fibres. Another hurdle is in finding data for transverse–longitudinal shear behaviour for yarns. This indicates a requirement for fundamental modelling of yarn behaviour. The authors are currently studying this problem as part of collaborative research.

## Acknowledgments

The work reported in this publication was carried out under the Technology Strategy Board's collaborative research and development programme, through Project No: TP/5/MAT/6/I/H0558C 'Multi-Scale Integrated Modelling for High Performance Flexible Materials'. The authors would like to thank Technology Strategy Board for financial support, and acknowledge the participation of the industrial and academic partners involved in this project: Unilever UK Central Resources, OCF PLC, Croda Chemicals Europe Ltd, University of Manchester, Heriot-Watt University, ScotCad Textiles Ltd, Carrington Career and Work wear Ltd, Moxon Ltd, Airbags international, Technitex Faraday Ltd.

## References

[1] Zeng X S, Shim V P W and Tan V B C 2006 Modelling inter-yarn friction in woven fabric armour *Int. J. Numer. Methods Eng.* **66** 1309–30

[2] Winterhalter C A, Teverovsky J, Wilson P, Slade J, Horowitz W, Tierney E and Sharma V 2005 Development of electronic textiles to support networks, communications, and medical applications in future US military protective clothing systems *IEEE Trans. Inform. Technol. Biomed.* **9** 402–6

[3] van Wyk C M 1946 Note on the compressibility of wool *J. Textile Inst.* **37** T285–92

[4] Toll S and Manson J A E 1994 An analysis of the compressibility of fibre assemblies *Proc. 6th Int. Conf. on Fibre-Reinforced Composites* (Newcastle Upon-Tyne: Institute of Materials) 25/1-25/10

[5] Robitaille F and Gauvin R 1998 Compaction of textile reinforcements for composites manufacturing: review of experimental results *Polym. Compos.* **19** 198–216

[6] Sherburn M 2007 Geometric and mechanical modelling of textiles *PhD Thesis* Nottingham University
[7] Cai Z and Gutowski T G 1992 The 3-d deformation behaviour of a lubricated fiber bundle *J. Compos. Mater.* **26** 1207–37
[8] Gutowski T G and Dillon G 1992 The elastic deformation of lubricated carbon fiber bundles: comparison of theory and experiments *J. Compos. Mater.* **26** 2330–47
[9] Komori T and Itoh M 1991 A new approach to the theory of the compression of fibre assemblies *Textile Res. J.* **61** 420–8
[10] Komori T and Itoh M 1991 Theory of the general deformation of fibre assemblies *Textile Res. J.* **61** 588–94
[11] Itoh M and Komori T 1991 An extension of the theory of the deformation of fibre assemblies *Sen'i Gakkaishi* **47** 563–72
[12] Lee D H and Carnaby G A 1992 Compressional energy of the random fibre assembly: I. Theory *Textile Res. J.* **64** 185–91
[13] Lee D H, Carnaby G A and Tandon S K 1992 Compressional energy of the random fibre assembly: II. Evaluation *Textile Res. J.* **62** 258–65
[14] Chen B X and Chou T W 1999 Compaction of woven fabric preforms in liquid composite moulding processes: single-layer deformation *Compos. Sci. Technol.* **59** 1519–26
[15] Lomov S V and Verpost I 2000 Compression of woven reinforcements: a mathematical model *J. Reinf. Plast. Compos.* **19** 1329–50
[16] Chen Z R, Ye L and Kruchenberg T 2006 A micromechanical compaction model for woven fabric preforms: I. Single layer *Compos. Sci. Technol.* **66** 3254–62
[17] Somashekar A A, Bicherton S and Bhattacharyya D 2006 An experimental investigation of non-elastic deformation for fibrous reinforcements in composites manufacturing *Composites A: Appl. Sci. Manuf.* **37** 858–67
[18] Kawabata S 1982 The development of the objective measurement of fabric handle *Proc. First Japan–Australia Symp. on Objective Specification of Fabric Quality, Mechanical Properties and Performance (Kyoto, Japan)* ed S Kawabata pp 31–59
[19] Reinhard T J, Dostal C A, Woods M S, Frissel H J and Ronke A W (ed) 1987 *Engineered Materials Handbook* (Materials Park, OH: ASM International)
[20] Hull D 1996 *An Introduction to Composite Materials* 2nd edn (Cambridge: Cambridge University Press)
[21] McBride T M 1997 The large deformation behaviour of woven fabric and microstructural evolution in formed textile composites *PhD Thesis* Boston University
[22] Boisse P, Gasser A and Hivet G 2001 Analysis of fabric tensile behaviour: determine of the biaxial tension-strain surfaces and their use in forming simulations *Compos. A: Appl. Sci. Manuf.* **32** 1395–414
[23] Mimaroglu A, Unal H and Arda T 2007 Friction and wear performance of pure and glass fibre reinforced poly-ether-imide on polymer and steel counterface materials *Wear* **262** 1407–13
[24] Crookston J J, Kari S, Warrior N A, Jones I A and Long A C 2007 3D Textile composite mechanical properties prediction using automated FEA of the unit cell *16th Int. Conf. Compos. Mater. (Japan)*
[25] Sadykova F Kh 1972 The Poisson ratio of textile fibres and yarns *Fibre Chem.* **3** 45–8
[26] Saunders R A, Lekakou C and Bader M G 1998 Compression and micro-structure of fibre plain woven cloths in the processing of polymer composites *Compos. A: Appl. Sci. Manuf.* **29** 443–54
[27] Chen B X, Lang E J and Chou T W 2001 Experimental and theoretical studies of fabric compaction behaviour in resin transfer moulding *Mater. Sci. Eng. A: Struct. Mater. Properties Microstruct. Process* **317** 188–96
[28] Kawabata S, Niwa M and Kawai H 1973 The finite-deformation theory of plain-weave fabrics: I. The biaxial-deformation theory *J. Textile Inst.* **64** 21–46